

## Article

# Patterns and Abundance of Rare Earth Elements in Sediments of a Bedrock River (Miño River, NW Iberian Peninsula)

Miguel Ángel Álvarez-Vázquez <sup>1,\*</sup> , Elena De Uña-Álvarez <sup>1</sup>  and Ricardo Prego <sup>2</sup> 

<sup>1</sup> Area of Physical Geography, GEAAT Research Group, Department of History, Art and Geography, University of Vigo, As Lagoas s/n, 32004 Ourense, Spain; edeuna@uvigo.es

<sup>2</sup> Instituto de Investigaciones Marinas (CSIC), Eduardo Cabello, 6, 36208 Vigo, Spain; prego@iim.csic.es

\* Correspondence: mianalva@uvigo.es

**Abstract:** Bedrock rivers, whose sedimentary geochemistry has been scarcely investigated, are suitable to test geochemical approaches in order to assess the existence and extent of human alterations in the natural abundance of rare earth elements. This work presents the study of REE contents in fine-grained sediments of the (bedrock) Miño River, in an urban reach of its middle course. Different statistical procedures were employed in order to decipher the abundances and patterns of distribution of REE in different environments, showing a higher REE accumulation in surface sediments trapped by potholes and other rock cavities. Background contents were estimated by iterative simple regression. After checking several possible reference elements, Y showed the highest potential for the series of REE from La to Lu. The regression result, namely background function, is very useful to minimize the effect of the natural variability in sediment contents. Background functions also allow for environmental assessment by the calculation of the so-called local enrichment factors. As a general conclusion, contamination, if it exists, is negligible in the area and low enrichments can be attributed to postdepositional processes related to organic matter and the geochemistry of Fe and Mn.



**Citation:** Álvarez-Vázquez, M.Á.; De Uña-Álvarez, E.; Prego, R. Patterns and Abundance of Rare Earth Elements in Sediments of a Bedrock River (Miño River, NW Iberian Peninsula). *Geosciences* **2022**, *12*, 105. <https://doi.org/10.3390/geosciences12030105>

Academic Editors: Pedro Dinis and Jesus Martinez-Frias

Received: 31 January 2022

Accepted: 20 February 2022

Published: 24 February 2022

**Publisher's Note:** MDPI stays neutral with regard to jurisdictional claims in published maps and institutional affiliations.



**Copyright:** © 2022 by the authors. Licensee MDPI, Basel, Switzerland. This article is an open access article distributed under the terms and conditions of the Creative Commons Attribution (CC BY) license (<https://creativecommons.org/licenses/by/4.0/>).

**Keywords:** lanthanoids; sediment; bedrock rivers; Miño/Minho River; NW Iberian Peninsula

## 1. Introduction

Chemical elements that can be found in relatively small contents in the earth's crust (trace elements, e.g., Au, Ag, Cu, Sn, Pb, Zn) have been used for a variety of purposes since the very beginning of human culture. The development of human technology has been increasing the number and quantity of these elements involved in human production systems, causing a side release to the environment.

Rare earth elements (REE) commonly include scandium, yttrium, and the lanthanoids. These elements have gained interest in the last decades due to their use in high-tech applications in fields such as industry, agriculture, and medicine. Between the many uses, they are present in manufacturing automotive catalytic converters (e.g., La, Ce), metallurgical additives and alloys (e.g., La, Ce, Pr, Nd, Y), glass and glass-polishing compounds (e.g., Ce, La, Pr, Nd, Gd, Er, Ho), ceramics (e.g., La, Ce, Pr, Nd, Y, Eu, Gd, Lu, Dy), magnets and power generation (e.g., Nd, Pr), displays and imaging (e.g., Eu, Y, Tb, Nd, Er, Gd), medical applications (e.g., Gd), [1–3], etc., to the point that REE are included between the so-called technology-critical elements (TCEs; [2]), or elements with a critical importance and increasing use in a variety of technological applications.

The consequences of the release of REE to the environment are still not well known [4,5]. Between the many environmental components, the composition of sediments is commonly used to track human impact and the nature–society relationships. Today, REE contamination is of increasing concern and was mainly addressed in sediments related to mining activities [6,7], and the use of fertilizers and their industry [8,9], among others. Given that under natural conditions REE contents highly depend on local mineralogy and lithology [1,10], geochemical procedures aimed to decouple the natural and human components [11,12]

developed for common contaminant trace elements should be tested for their potential application to REE.

In this regard, river sediments are of particular interest, because rivers are principal receivers of human byproducts and wastes. Moreover, they usually host important population settlements and industrial facilities. Thus, river sediments, receivers of the human footprint, host a registry of the human-nature relationships. Usually, works on anthropogenic imprints in fluvial sediments are performed in estuaries and well-developed floodplains with an abundance of fine sediments, e.g., [13,14]. However, small rivers [15], headwater rivers, or bedrock rivers were barely addressed in scientific literature. The importance of these watercourses is probably underestimated, e.g., Chakrapani [16] said that small rivers drain about a 20% of the continents, and Whipple et al. [17] pointed to bedrock rivers, i.e., rivers where the bedrock is exposed or there is a relatively thin layer of sediments as intense modelers of the continental crust. These three types of rivers share the characteristics of a low accumulation of sediments, particularly fine sediments; this is perhaps one of the reasons for the scarcity of geochemical studies in this kind of environment. Miller et al. [18] asserted that in bedrock rivers, the geochemistry of the chemically reactive fine fraction of sediments is still very unknown.

In previous works exploring fluvial potholes and other sculpted forms in bedrock rivers [19,20], the capacity of rock cavities to retain sediments was evidenced, which raised the question of how contaminants accumulate in these peculiar microenvironments. It also explored their utility as sediment traps [21]. In consequence, this work was aimed at exploring patterns and the abundance of REE in fluvial sediments of rivers with low sediment accumulation. To conduct this, an urban reach of the Miño River (NW Iberian Peninsula) was selected, where three major sediment-accumulation microenvironments were identified, i.e., (i) surface sediments located in the riverbanks (such as small beaches and sand bars); (ii) surface sediments trapped by fluvial sculpted forms [22], which are commonly removed during high waters and deposited during the dry season; and (iii) consolidated permanent sediments inside depth potholes (>40 cm [19]). The three microenvironments were examined to see differences or similitudes in the REE accumulation patterns. Last but not the least, background estimation was tested to perform a proper environmental assessment of the measured REE.

## 2. Study Area

The Miño River (Minho in Portugal) is the main watercourse in the NW Iberian Peninsula. The river (Figure 1) flows along 315.5 km from its birth (Serra de Meira, Spain, 700 m a.s.l.) to its mouth in the Atlantic Ocean (between the localities of A Guarda, Spain, and Caminha, Portugal). Its fluvial network drains 18,080 km<sup>2</sup> mainly over the bedrock, following a general NE–SW direction. The majority of the main channel and tributaries can be classified as bedrock rivers according to Whipple et al. [15].

The middle sector of the river belongs to the Galicia-Trás-os-Montes Zone of the Iberian Massif, where Variscan granites are dominant, intruding mica-schists, quartz-schists and feldspathic schists [23]. Granites (felsic rocks with a content in Si > 70%) are dominant in the study area. They include granodiorites (calc-alkaline series) with coarse-porphyritic grain, rich in quartz, K-feldspar (microcline) and plagioclase feldspar (anortite) with biotite having a low content of Fe and Mg oxides; two-mica granites (alkaline series) with medium-coarse grain, rich in quartz; and plagioclase feldspar (albite) and biotite, which more than muscovite, are calcium scarce and Al<sub>2</sub>O<sub>3</sub> abundant. Both types have apatite and zircon as secondary minerals. Minority schists are composed of quartz, biotite, and muscovite. Quartz dikes, aplite dykes, and veins (quartz, K-feldspar, and acid plagioclase) are present.

Near the town of Ourense, the Miño presents a deep incision (about 400 m, flowing across a tectonic depression). Samples were withdrawn in an urban river reach (Figure 1) of about 4 km long and an increased widening from upstream (75 m) to downstream (395 m). The river flows through a relatively flat terrain (about 1% slope) over igneous rocks. There is a sequential presence of exposed rock outcrops, boulders, pebbles, and sand with the

increased widening. The reach is highly modified by human activities, i.e., the Ourense (105,643 inhab. in 2020), households, small industries, roads, bridges, and promenades and dams.

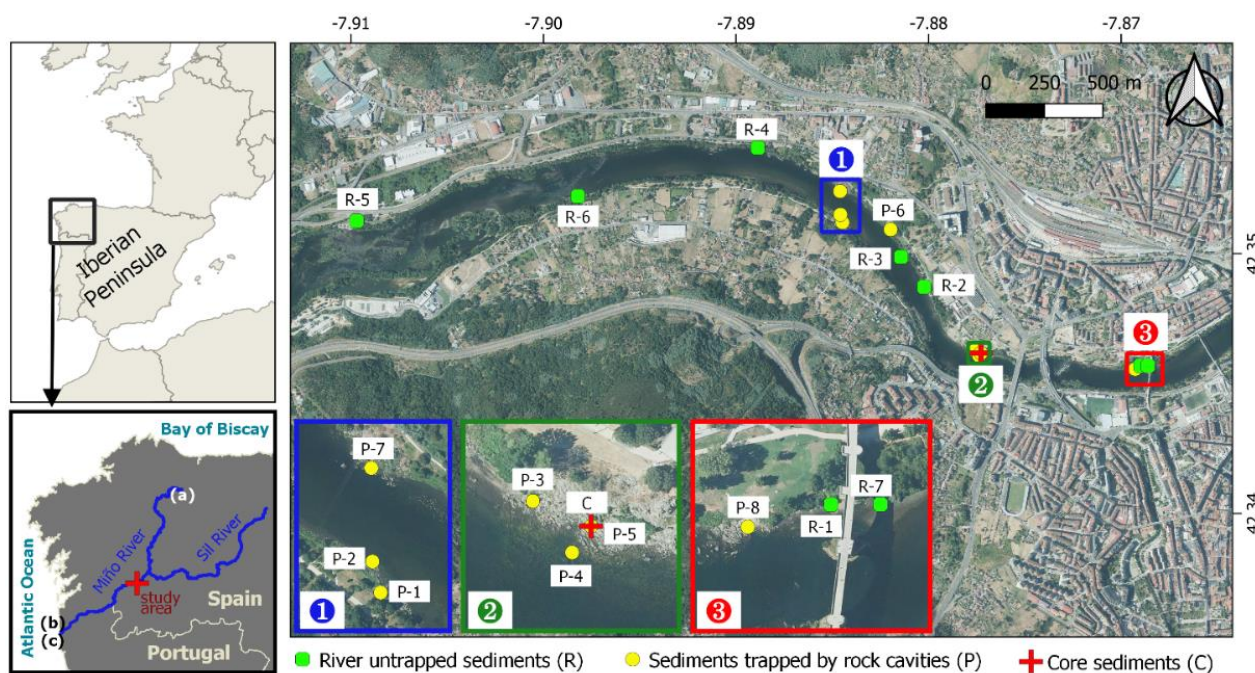


**Figure 1.** Location map of the study area and samples position, (a) indicates the springs of the Miño River in Serra de Meira, (b) and (c) are the localities of A Guarda (Spain) and Caminha (Portugal), respectively. Basemap aerial orthophoto from the Spanish-PNOA (©IGN).

Previous studies in this urban reach [19,20,24] and the corresponding fieldwork pointed out that the fluvial sculpted forms (potholes, furrows, scallops) have the capacity to trap sediments in an area where sedimentation is scarce. Particularly, the rounded potholes can host permanent deposits when the depth reaches 40 cm [19], but all rock cavities that flank the channel can retain sediments of different thickness, particularly during low flow periods. Besides this, surface sediments are deposited in the channel margins of the river.

### 3. Materials and Methods

Fluvial sediments were sampled in the riverbanks. Three differentiated microenvironments were considered: (i) surface sediments (eight samples: P-1 to P-8) trapped inside potholes and other rock cavities (Figure 2a–c), (ii) a 22 cm core of permanent sediments trapped in a pothole (Figure 2d), 2 cm layers (samples C-1 to C-11) and, (iii) seven river surface sediments (Figure 2e) not trapped in rock cavities (samples R-1 to R-7). The sample location is presented in Figure 1. The sediment samples were carefully collected with a plastic spatula and stored in plastic zip bags. Samples were further on laboratory dried ( $45 \pm 5$  °C until constant weight) and sieved through a 0.063 mm mesh. The fine fraction (<0.063 mm) was selected for analysis.

The chemical analysis was commissioned to the Center for Scientific and Technological Research Support (CACTI–University of Vigo), an ISO 9001 certified laboratory. Six potentially explanatory variables (contents of Al, Fe, Rb, Li, Sc, and Y) were selected for being common reference elements in sediment geochemistry [25–27]. These elements were determined by inductively coupled plasma optical emission spectrometry (ICP-OES) and the lanthanoids (La, Ce, Pr, Nd, Sm, Eu, Gd, Tb, Dy, Ho, Er, Tm, Yb, and Lu) by inductively coupled plasma mass spectrometry (ICP-MS). Promethium (Pm) was not considered due to its very low content in the earth’s crust. The contents of Pr, Eu, and Tb in sediments were

calculated by the internal calibration of the instrument, due to the absence of a calibration standard.

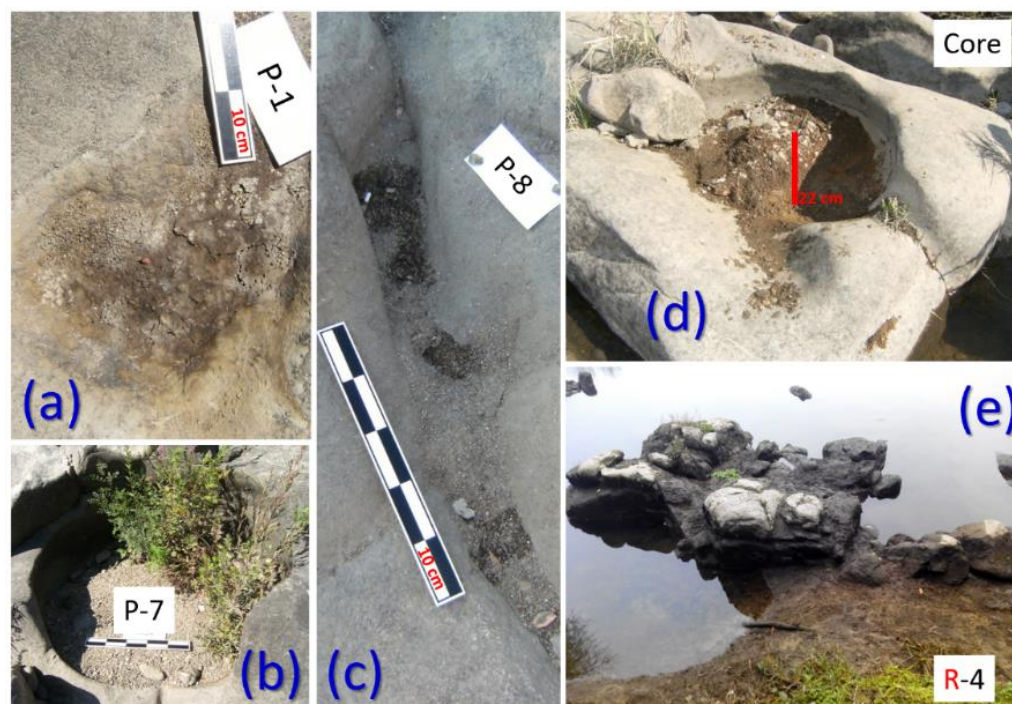


**Figure 2.** Examples of the sampled sediments, (a–c) correspond to surface sediments trapped by rock cavities (P), (d) is the sediment core (C) in the moment of sampling, and (e) corresponds to untrapped fluvial sediments (R).

The International Union of Pure and Applied Chemistry (IUPAC) consider a group formed by Sc, Y, and 15 lanthanoids (La, Ce, Pr, Nd, Pm, Sm, Eu, Gd, Tb, Dy, Ho, Er, Tm, Yb, and Lu), as rare earth elements (REE) (see previous note on Pm). When only including lanthanoids (Ln), it is advisable to note it as Ln-REE. At the same time, it is a common subdivision into light REE (LREE: La, Ce, Pr, Nd, Sm, Eu, and Gd), and heavy REE (HREE: Tb, Dy, Ho, Er, Tm, Yb, and Lu), also following the IUPAC recommendations. However, there is still some scientific consensus lacking about this last classification, but this nomenclature is the one that will be used in this work.

Consequently, the normalized LREEs/HREEs ( $L_N/H_N$ ) can be defined as:

$$L_N/H_N = (La_N + Ce_N + Pr_N + Nd_N + Sm_N + Eu_N + Gd_N)/(Tb_N + Dy_N + Ho_N + Er_N + Tm_N + Yb_N + Lu_N) \quad (1)$$

where the European shale (ES, [28]) was used to normalize each lanthanoid, dividing its content in the sediment sample by the respective content in ES. Values higher than 1 denote LREE enrichment; conversely, values lower than 1 mean HREE enrichment.

Anomalies of Ce and Eu ( $Ce/Ce^*$  and  $Eu/Eu^*$ ) were used to highlight depletion or enrichment of these elements. They were calculated according to McLennan [29]:

$$Eu/Eu^* = Eu_N/(Sm_N \cdot Gd_N)^{0.5} \quad (2)$$

$$Ce/Ce^* = Ce_N/(La_N \cdot Pr_N)^{0.5} \quad (3)$$

where  $La_N$ ,  $Ce_N$ ,  $Pr_N$ ,  $Sm_N$ ,  $Eu_N$ , and  $Gd_N$  were the contents of each element normalized (divided) by their contents in the European shale [28]. Values above 1 denote positive anomalies, whereas values below 1 denote negative anomalies. These anomalies should be greater than  $\approx 5\%$  to be considered significant [29].

The dataset was processed with the Statgraphics Centurion 18 software (© Statgraphics Technologies, Inc., The Plains, VA, USA).

## 4. Results and Discussion

### 4.1. Ln-REE Abundance

Exploring the data distribution of REE (16 variables and 26 samples), the standard skewness and kurtosis showed, in general, values within the range of  $-2$  to  $+2$ . These results point to a normal distribution in the contents in sediments. There were three exceptions where the standard skewness was  $>2$ , to wit, La (2.04), Pr (2.36), and Nd (2.05); the standard kurtosis was also above 2 for Pr (2.17). Checking the data, these violations of the normal distribution were caused by a single sample (P-1), which presents contents identified as outliers (outside Tukey's inner fences) for these three elements, i.e., La ( $162 \text{ mg kg}^{-1}$ ), Pr ( $39 \text{ mg kg}^{-1}$ ), and Nd ( $124 \text{ mg kg}^{-1}$ ), but also for Ce ( $367 \text{ mg kg}^{-1}$ ), Sm ( $26 \text{ mg kg}^{-1}$ ), Gd ( $32 \text{ mg kg}^{-1}$ ), and Dy ( $8.8 \text{ mg kg}^{-1}$ ). When outliers are excluded from the distribution test, the standard skewness and kurtosis for all the variables (between  $-2$  and  $+2$ ) pointed to a normal distribution of the dataset. In consequence, parametric statistics were selected for description and the dataset is characterized in Table 1.

**Table 1.** Summarized REE contents ( $\text{mg kg}^{-1}$ ) in the studied sediments. All correspond to the complete datasets (statistics after deleting outliers), P are surface sediments trapped into rock cavities, C is the depth core trapped into a pothole, and R are untrapped sediments in the riverbanks. The EU shale are the reference contents from [28].

	All	P	C	R	EU Shale
Sc	$2.21 \pm 0.28$	$2.00 \pm 0.16$	$2.40 \pm 0.24$	$2.15 \pm 0.27$	$16^1$
Y	$20.2 \pm 2.6$	$20.5 \pm 1.5$	$21.8 \pm 1.7$	$17.2 \pm 2.2$	31.9
La	$95.9 \pm 17.8$	$121.2 \pm 21.2$	$93.6 \pm 8.1$	$80.0 \pm 14.8$	44.3
Ce	$229 \pm 37$	$276 \pm 45$	$224 \pm 20$	$204 \pm 42$	88.5
Pr	$22.3 \pm 4.2$	$28.4 \pm 5.1$	$21.8 \pm 2.2$	$18.5 \pm 2.9$	10.6
Nd	$74.8 \pm 13.1$	$93.4 \pm 15.7$	$74.2 \pm 5.8$	$61.4 \pm 9.2$	39.5
Sm	$15.8 \pm 2.6$	$19.5 \pm 3.1$	$15.8 \pm 1.2$	$13.0 \pm 1.7$	7.30
Eu	$2.67 \pm 0.70$	$3.12 \pm 0.96$	$2.93 \pm 0.21$	$1.97 \pm 0.49$	1.48
Gd	$20.0 \pm 3.6$	$24.6 \pm 4.3$	$20.1 \pm 1.5$	$16.2 \pm 2.5$	6.34
Tb	$1.29 \pm 0.41$	$1.68 \pm 0.39$	$1.23 \pm 0.33$	$0.95 \pm 0.10$	0.944
Dy	$5.94 \pm 0.90$	$6.90 \pm 1.06$	$6.20 \pm 0.44$	$4.86 \pm 0.48$	5.86
Ho	$0.919 \pm 0.146$	$1.036 \pm 0.149$	$0.940 \pm 0.066$	$0.752 \pm 0.068$	1.17
Er	$2.33 \pm 0.32$	$2.56 \pm 0.27$	$2.42 \pm 0.18$	$1.95 \pm 0.17$	3.43
Tm	$0.231 \pm 0.032$	$0.248 \pm 0.030$	$0.243 \pm 0.017$	$0.194 \pm 0.018$	0.492
Yb	$1.06 \pm 0.14$	$1.13 \pm 0.12$	$1.11 \pm 0.08$	$0.89 \pm 0.07$	3.26
Lu	$0.212 \pm 0.031$	$0.227 \pm 0.031$	$0.224 \pm 0.015$	$0.177 \pm 0.020$	0.485
Ln-REEs	$472 \pm 79$	$580 \pm 96$	$465 \pm 39$	$405 \pm 73$	214
LREEs	$461 \pm 77$	$567 \pm 94$	$453 \pm 38$	$395 \pm 73$	198
HREEs	$12.1 \pm 2.0$	$13.8 \pm 2.0$	$12.4 \pm 0.9$	$9.8 \pm 0.9$	15.6
$L_N/H_N$	$3.2 \pm 0.2$	$3.3 \pm 0.2$	$3.1 \pm 0.1$	$3.2 \pm 0.3$	1
Ce/Ce*	$1.21 \pm 0.07$	$1.16 \pm 0.08$	$1.22 \pm 0.03$	$1.29 \pm 0.06$	1
Eu/Eu*	$0.70 \pm 0.10$	$0.65 \pm 0.15$	$0.76 \pm 0.05$	$0.62 \pm 0.08$	1

<sup>1</sup> The content of Sc is not provided for the EU shale, so it was included in the value of the Post Archean Australian shale (PAAS, [30]).

Compared with the global reference of the EU shale [28], coherent also with data from eroded granites [31], Y, Tb, Dy, Ho, Er, Tm, and Lu presented comparable contents; La, Ce, Pr, Nd, Sm, Eu, and Gd are enriched at least in a factor of 2, and Yb is depleted (detailed data in Table 1). In general, it can be said that LREEs were enriched. This statement was confirmed by the  $L_N/H_N$  index always having values above 1, with a range from 2.8 to 3.6. Given that the contents corresponded to the silt-clay fraction, this enrichment was coherent with observations in clayed soils [32], presenting enrichment in LREEs, whereas HREEs were more associated with refractory minerals in sandy soils. Particularly,

Bayon et al. [33] pointed to the clay fraction, which is “systematically characterized by a progressive enrichment from the heavy to the light REE”. In the sediments under study, a positive anomaly of Ce ( $Ce/Ce^*$  from 1.1 to 1.4) and a negative anomaly of Eu ( $Eu/Eu^*$  from 0.5 to 0.9) was also observed. Both LREE enrichment and Ce and Eu anomalies were reported ( $L_N/H_N = 3.28$ ,  $Ce/Ce^* = 2.26$  and  $Eu/Eu^* = 0.44$ ; [31]) in fluvial sediments and soils formed by granite weathering products. The Eu positive anomaly was also characteristic of the clay fraction of sediments [30].

Figure 3 presents the normalized patterns of Ln-REE in the three subsets (P, C, and R) compared with a previous work [34] in the low Miño River. The general pattern in the urban reach under study responded to what was described above, i.e., general enrichment of LREE and depletion of HREE compared to the ES [28]. This pattern is similar to that presented by Bayon et al. [33] for the clay fraction of rivers draining igneous/metamorphic terranes. European shale-normalized contents of Gd presented a peak in the studied sediments, which could be due to any natural factor because an anthropogenic source is not probable. Although contamination by Gd has been reported in fluvial waters [3,35] due to its use in medical applications, this element tends to remain in solution and is not incorporated into the sediments. Compared with the main channel and tributaries of the lower reach of the Miño River, the main differences may be caused by the sediment fraction analyzed (<2 mm in the low Miño, [34]). However, in the main channel (aL and bL), the same pattern of higher normalized contents of LREE was observed. The Gd peak content was also observed in the Gadanha (Ga) and Tea (Te) tributaries, but not in the main channel; thus, it could be related with local lithological complexities.

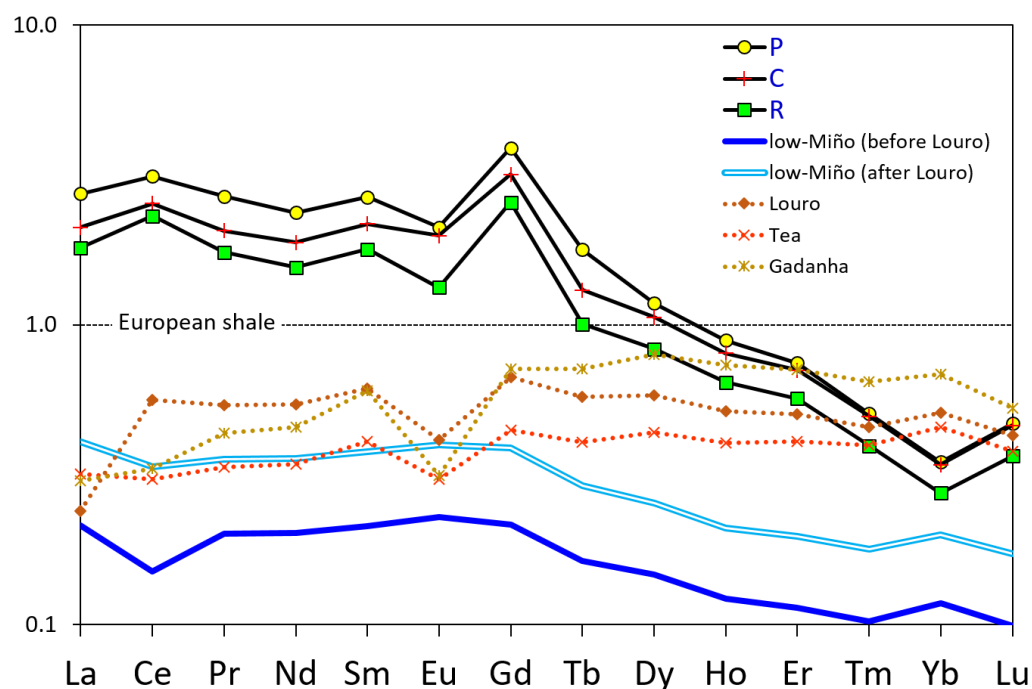


**Figure 3.** European shale [28] normalized patterns (logarithmic scale) of Ln-REE in sediments of the sampled section of the Miño River according to its origin (P: surface sediments trapped into rock cavities; C: sediment depth core trapped into a pothole; R: untrapped surface river sediments). Data from the lower course of Miño River [34] was provided for comparison (main channel before and after the Louro River, a known source of REE, and three tributaries of the low Miño, i.e., Tea, Louro, and Gadanha Rivers).

#### 4.2. Depositional Microenvironments

As seen in Figure 3, there were no remarkable differences in the variation of the normalized pattern between surface sediments trapped by rock cavities (P), core sediments trapped into a pothole (P), and untrapped river sediments (R). Aimed to check similarities

and differences between the three major microenvironments accumulating sediments in bedrock rivers (P, C, and R), statistical tests were performed to identify statistical significant differences in the contents of the three data subsets. In general, average contents were higher in surface sediments trapped by rock cavities and the lower contents were found in accumulations of fluvial sediments not trapped by potholes or furrows (Table 1). The variance of the data (ANOVA) was tested into two components (between-group and within-group). The p-value of the F-test (ratio of the between-group estimate to the within-group estimate) was always below 0.05; this means that for all the variables, there was a significant difference between the means of the 3 subsets at the 95% confidence level. Consequently, differences existed in the deposition accumulation patterns of REEs in sediments trapped by rock cavities or accumulated in the riverbanks, pointing to a higher accumulation inside rock cavities than in untrapped sediments. Notwithstanding, the  $L_N/H_N$  ratio did not show a statistically significant difference (95% confidence level) between the means of the three subsets (see Table 1). Thus, the small difference might be marked by single elements.

A multiple range test (Fisher's least significant difference procedure) was used to see which subgroup means (P, C, and R) were significantly different from which others. (i) Five variables (i.e., Nd, Sm, Gd, Dy, and Ho) discriminated three different homogeneous groups. Thus, there was a statistically significant difference between the means of the three subgroups at the 95% confidence level. (ii) Six variables (i.e., Y, Eu, Er, Tm, Yb, and Lu) separated two homogeneous groups, i.e., fluvial untrapped sediments (R) from those trapped into rock cavities (P and C). Conversely, (iii) La, Ce, Pr, and Tb also identified two homogeneous groups, but separated the surface sediments trapped into shallow sculpted forms (P) from those obtained in the riverbanks (S) and the core (C). Although there was a general accumulation pattern of REEs responding to  $P > C > R$ , there was a differentiated response to the microenvironment complexities, the contents of trapped sediments (P and C) always being higher than those in untrapped sediments (R). Therefore, rock cavities seemed to act as an REEs trap, increasing their contents in sediments. The accumulation pattern classification of REEs can be summarized as follows:

1.  $P > C > R$  (Nd, Sm, Gd, Dy, and Ho)
2.  $P \approx C > R$  (Y, Eu, Er, Tm, Yb, and Lu)
3.  $P > C \approx R$  (La, Ce, Pr, and Tb)

The sediments of bedrock rivers are middle members of the weathering and erosion process, in this case, of granites. Chen et al. [31] considered REE migration processes from uplands to lowlands presenting enrichments in terminal paddy fields. In this line, the higher contents inside rock cavities could be attributed to a lower loss by leaching or an increased precipitation inside cavities, potholes, and other sculpted forms, which are semienclosed systems flooded during high waters and dried by evaporation in the dry season. The accumulation or retention seemed to be more intense in the surface sediments of rock cavities and could be related with retention during the development of coatings and biofilms, favored by the moisture and the intensity of sunlight, as previously observed for other trace elements [21]. As an example, see the crust formed in the sample P-1 (Figure 2a). This sample showed the highest contents of the complete dataset for La ( $162 \text{ mg kg}^{-1}$ ), Ce ( $367 \text{ mg kg}^{-1}$ ), Pr ( $38.7 \text{ mg kg}^{-1}$ ), Nd ( $125 \text{ mg kg}^{-1}$ ), Sm ( $25.7 \text{ mg kg}^{-1}$ ), Gd ( $32.5 \text{ mg kg}^{-1}$ ), Dy ( $8.83 \text{ mg kg}^{-1}$ ), Ho ( $1.29 \text{ mg kg}^{-1}$ ), Er ( $3.02 \text{ mg kg}^{-1}$ ), Tm ( $0.29 \text{ mg kg}^{-1}$ ), Yb ( $1.33 \text{ mg kg}^{-1}$ ), and Lu ( $0.27 \text{ mg kg}^{-1}$ ). Most of the aforementioned were identified as outliers in the data distribution. Note that nonterrestrial fractions, i.e., organic matter and Fe–Mn oxyhydroxides, can host significant quantities of REEs [30]. Moreover, Miller et al. [16] also pointed to the formation of Fe–Mn oxyhydroxides to explain enrichment in trace metals downstream cascades in a bedrock river.

#### 4.3. Background Estimation and Environmental Assessment

When assessing human impact in sediments, a critical step is to estimate the natural background level [25]. This issue was broadly considered in the case of common contaminant trace elements (e.g., Cu, Ni, Pb, Zn). According to the IUPAC definition of

a trace element, Ln-REE can be considered within this group because, in general, their contents are below  $100 \text{ mg kg}^{-1}$ . Between the many techniques developed to estimate the background of trace elements [11,12], the calculation of background functions using a reference (conservative) element at the local scale is recommended [25,36].

In order to test the appropriateness of this procedure in the case of lanthanoids, six common reference elements [25–27] were considered (i.e., Al, Fe, Li, Rb, Sc and Y). The correlation (Pearson product–moment correlations) between reference elements and Ln-REE was checked to identify the reference elements with a higher potential. Between the preselected, Y presented the best potential. It was directly correlated (statistically significance level 0.01, bilateral) with La (0.52), Pr (0.53), Nd (0.57), Sm (0.58), Eu (0.77), Gd (0.63), Dy (0.76), Ho (0.79), Er (0.85), Tm (0.91), Yb (0.89), and Lu (0.91); the correlation was weaker, but also significant (level 0.05, bilateral), with Ce (0.48) and Tb (0.47). The other reference elements do not present relevant results, only weak correlations between Al and Lu (0.41), Li and Tm (0.41), Li and Yb (0.42), Li and Lu (0.43), Sc and Ce (-0.43), and Sc and Tb (-0.41). Thus, Y was selected for further procedures.

The background, in the form of a background function, was estimated by simple least squares regression between Y (the independent variable) and any single Ln-REE (the dependent variable). These equations took the general shape of a straight line, with intercept = 0 in this case, i.e., “ $y = ax$ ”, where “ $y$ ” is the theoretical background content of a given element (denoted further as  $[El]_{BG}$ ), “ $a$ ” is a constant and “ $x$ ” is the measured content of the reference element (hereinafter [Y]). These equations allowed estimating the background of any single element for each sample as a function of the content of the reference element [12,25]. The equations were obtained after iterative simple regression, i.e., consecutive regressions deleting unusual residuals in each step. Unusual residuals were studentized residuals with an absolute value higher than 2, or what is the same when the measured value differed more than 2 standard deviations from the model. The results are summarized in Table 2, and some examples are presented in Figure 4.

**Table 2.** Results of the background (BG) equations obtained by least squares iterative simple regression.  $R^2$  is the coefficient of determination,  $n$  is the number of samples included in the regression, and BG is the estimated background content from the samples included in the regression.

	BG-Equation	$R^2$	$n$	BG
La	$[La]_{BG} = 4.2981[Y]$	0.911	14	$88.5 \pm 12.4$
Ce	$[Ce]_{BG} = 10.487[Y]$	0.747	16	$217 \pm 27$
Pr	$[Pr]_{BG} = 1.0038[Y]$	0.831	16	$20.5 \pm 3.0$
Nd	$[Nd]_{BG} = 3.456[Y]$	0.852	15	$71.9 \pm 7.9$
Sm	$[Sm]_{BG} = 0.7352[Y]$	0.877	15	$15.3 \pm 1.6$
Eu	$[Eu]_{BG} = 0.1331[Y]$	0.758	18	$2.72 \pm 0.45$
Gd	$[Gd]_{BG} = 0.9265[Y]$	0.923	14	$19.3 \pm 2.3$
Tb	REGRESSION NOT SATISFACTORY (best $R^2 = 0.227$ )			
Dy	$[Dy]_{BG} = 0.2869[Y]$	0.977	14	$5.81 \pm 0.68$
Ho	$[Ho]_{BG} = 0.0433[Y]$	0.965	17	$0.87 \pm 0.10$
Er	$[Er]_{BG} = 0.1115[Y]$	0.949	17	$2.23 \pm 0.26$
Tm	$[Tm]_{BG} = 0.0113[Y]$	0.937	21	$0.22 \pm 0.03$
Yb	$[Yb]_{BG} = 0.0516[Y]$	0.941	18	$1.04 \pm 0.12$
Lu	$[Lu]_{BG} = 0.0103[Y]$	0.956	21	$0.20 \pm 0.03$

The obtained background functions presented a good coefficient of determination ( $R^2$ ), from 0.747 (Ce) to 0.977 (Dy). The exception is Tb; the regression with Y (also checked with Sc) did not produce an acceptable correlation. It is important to note that most of the unusual residuals discriminated by the iterative regression belonged to surface samples trapped by rock cavities, and more or less were coincident in the same samples for all the variables. The contents of these cases were higher than expected, reinforcing the idea of any surface factor retaining or accumulating Ln-REE probably not being related with human inputs because it was observable for all the Ln-REE in a higher or lesser extent.

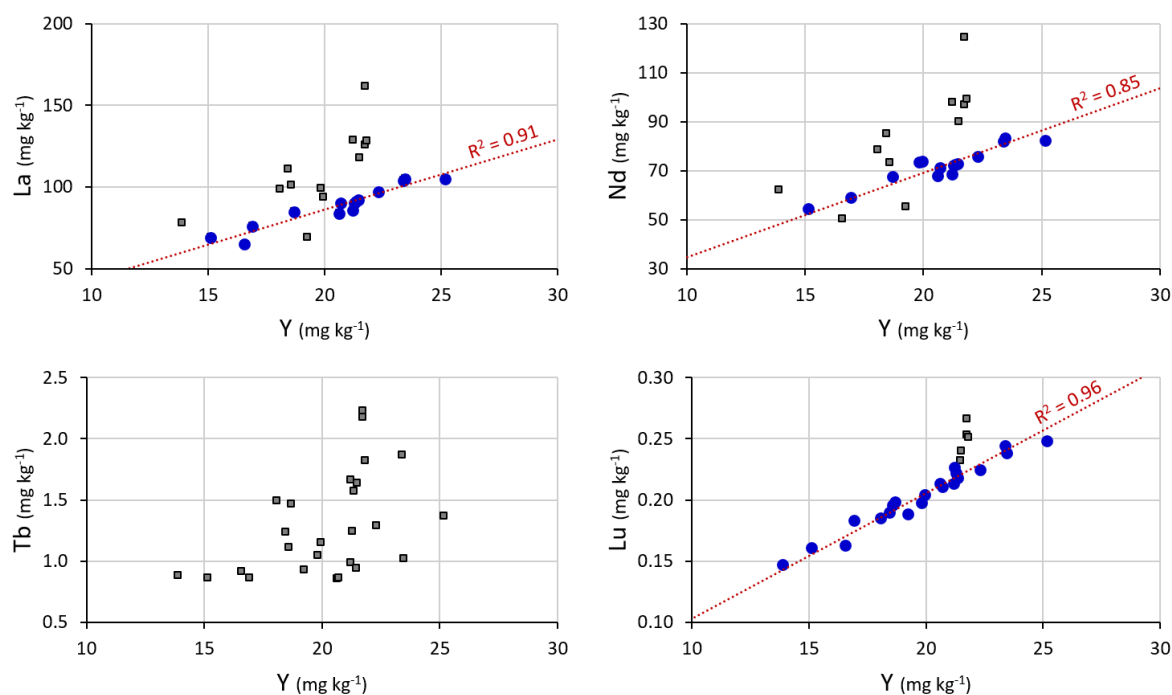


**Figure 4.** Examples of regression results (least squares simple regression with intercept = 0) between Y (independent variable) and lanthanoids (dependent variable). Blue dots are the samples included in the regression, gray squares are samples identified as unusual residuals, and the red dotted line is the regression model.

Once the background functions were obtained, the contamination assessment was performed by the use of the local enrichment factor (LEF; [25]). This index calculated the quotient between the measured content of any element ( $[EI]$ ) divided by the estimated background content from the background equation ( $[EI]_{BG}$ ). The results corroborated the absence of human alterations. None of the samples presented a LEF > 2, the common threshold to separate contamination from natural variability. Even with the aforementioned sample P-1, which presented the higher contents and also the higher LEFs, none of them were above 1.8 (La = 1.7, Ce = 1.6, Pr = 1.8, Nd = 1.7, Sm = 1.6, Eu = 1.3, Gd = 1.6, Dy = 1.4, Ho = 1.4, Er = 1.2, Tm = 1.2, Yb = 1.2, Lu = 1.2).

## 5. Conclusions

Rare earth element contents in sediments accumulated in the channel and riverbanks of the Miño River (in the reach under study) were characterized and the results were presented for further comparison. Differences existed between the three microenvironments under study: i.e., surface sediments trapped into rock cavities, pothole-trapped depth core sediments, and untrapped sediments in the riverbanks. These differences were proven by the statistical analysis. It was observed that surface sediments trapped into rock cavities tended to accumulate more REE than riverbank untrapped sediments. Processes taking place within the sediments, such as bioactivity (organic matter) and the formation of Fe and Mn oxyhydroxides, could be more intense in rock cavities flooded during the wet season and dried by evaporation during the dry season. To estimate the local background of REE, some possible reference (lithogenic) elements were tested. Yttrium showed higher potential as a normalizing element. The background was estimated by iterative least squares simple regression, where Y was the independent variable and each single element the dependent variable. The result of the background was in the form of a straight line with intercept = 0 ( $y = ax$ ). Instead of providing a single content value, the background function allowed the calculation of the estimated background for each sample, taking into account the natural variation in sediment content. The background functions also allowed

for the calculation of local enrichment factors (LEFs), a commonly employed strategy in environmental assessment. The results of the LEFs for each sample, together with the previous discussion of the data, contribute to the conclusion of a negligible contamination in the area. Minor enrichments can be attributed to naturally occurring processes. The results are promising in applying regression to estimate REE background and local enrichment factor to assess contamination. However, research is still needed and the procedure needs to be corroborated for different areas, different lithologies, and with a much higher number of samples. Research will continue in this line.

**Author Contributions:** Conceptualization, E.D.U.-Á., R.P. and M.Á.Á.-V.; methodology, M.Á.Á.-V. and E.D.U.-Á.; sampling and fieldwork, M.Á.Á.-V. and E.D.U.-Á.; data curation, R.P. and M.Á.Á.-V.; writing—original draft preparation, M.Á.Á.-V.; writing—review and editing, E.D.U.-Á. and R.P.; funding acquisition, M.Á.Á.-V. and E.D.U.-Á. All authors have read and agreed to the published version of the manuscript.

**Funding:** This research was funded by the Universidade de Vigo and Diputación de Ourense, grant number INOU15-02. M.A. Álvarez-Vázquez was supported by the Xunta de Galicia through the postdoctoral grant #ED481B-2019-066.

**Institutional Review Board Statement:** Not applicable.

**Informed Consent Statement:** Not applicable.

**Conflicts of Interest:** The authors declare no conflict of interest.

## References

- Balaram, V. Rare earth elements: A review of applications, occurrence, exploration, analysis, recycling, and environmental impact. *Geosci. Front.* **2019**, *10*, 1285–1303. [[CrossRef](#)]
- Cobelo-García, A.; Filella, M.; Croot, P.; Frazzoli, C.; Du Laing, G.; Ospina-Alvarez, N.; Rauch, S.; Salaun, P.; Zimmermann, S. COST action TD1407: Network on technology-critical elements (NOTICE)—from environmental processes to human health threats. *Environ. Sci. Pollut. Res.* **2015**, *22*, 15188–15194. [[CrossRef](#)] [[PubMed](#)]
- Migaszewski, Z.M.; Gałuszka, A. The characteristics, occurrence, and geochemical behavior of rare earth elements in the environment: A review. *Crit. Rev. Environ. Sci. Technol.* **2015**, *45*, 429–471. [[CrossRef](#)]
- Gu, Y.G.; Gao, Y.P.; Huang, H.H.; Wu, F.X. First attempt to assess ecotoxicological risk of fifteen rare earth elements and their mixtures in sediments with diffusive gradients in thin films. *Water Res.* **2020**, *185*, 116254. [[CrossRef](#)] [[PubMed](#)]
- Rim, K.T. Effects of rare earth elements on the environment and human health: A literature review. *Toxicol. Environ. Health Sci.* **2016**, *8*, 189–200. [[CrossRef](#)]
- Liu, W.S.; Guo, M.N.; Liu, C.; Yuan, M.; Chen, X.T.; Huot, H.; Zhao, C.M.; Tang, Y.T.; Morel, J.L.; Qiu, R.L. Water, sediment and agricultural soil contamination from an ion-adsorption rare earth mining area. *Chemosphere* **2019**, *216*, 75–83. [[CrossRef](#)] [[PubMed](#)]
- Romero-Freire, A.; Minguez, L.; Pelletier, M.; Cayer, A.; Caillet, C.; Devin, S.; Gross, E.M.; Guérol, F.; Pain-Devin, S.; Vignati, D.A.L.; et al. Assessment of baseline ecotoxicity of sediments from a prospective mining area enriched in light rare earth elements. *Sci. Total Environ.* **2018**, *612*, 831–839. [[CrossRef](#)]
- Sanders, L.M.; Luiz-Silva, W.; Machado, W.; Sanders, C.J.; Marotta, H.; Enrich-Prast, A.; Bosco-Santos, A.; Boden, A.; Silva-Filho, E.V.; Patchineelam, S.R. Rare earth element and radionuclide distribution in surface sediments along an estuarine system affected by fertilizer industry contamination. *Water Air Soil Pollut.* **2013**, *224*, 1742. [[CrossRef](#)]
- Costa, L.; Mirlean, N.; Johannesson, K.H. Rare earth elements as tracers of sediment contamination by fertilizer industries in Southern Brazil, Patos Lagoon Estuary. *Appl. Geochem.* **2021**, *129*, 104965. [[CrossRef](#)]
- Prego, R.; Caetano, M.; Bernárdez, P.; Brito, P.; Ospina-Alvarez, N.; Vale, C. Rare earth elements in coastal sediments of the northern Galician shelf: Influence of geological features. *Cont. Shelf Res.* **2012**, *35*, 75–85. [[CrossRef](#)]
- Dung, T.T.T.; Cappuyns, V.; Swennen, R.; Phung, N.K. From geochemical background determination to pollution assessment of heavy metals in sediments and soils. *Rev. Environ. Sci. Bio/Technol.* **2013**, *12*, 335–353. [[CrossRef](#)]
- Birch, G.F. Determination of sediment metal background concentrations and enrichment in marine environments—a critical review. *Sci. Total Environ.* **2017**, *580*, 813–831. [[CrossRef](#)] [[PubMed](#)]
- Tůmová, Š.; Hruběšová, D.; Vorm, P.; Hošek, M.; Grygar, T.M. Common flaws in the analysis of river sediments polluted by risk elements and how to avoid them: Case study in the Ploučnice River system, Czech Republic. *J. Soils Sediments* **2019**, *19*, 2020–2033. [[CrossRef](#)]
- Álvarez-Vázquez, M.Á.; González-Prieto, S.J.; Prego, R. Possible impact of environmental policies in the recovery of a Ramsar wetland from trace metal contamination. *Sci. Total Environ.* **2018**, *637*, 803–812. [[CrossRef](#)] [[PubMed](#)]
- Meybeck, M.; Friedrich, G.; Thomas, R.; Chapman, D. Rivers. In *Water Quality Assessments—A Guide to Use of Biota, Sediments and Water in Environmental Monitoring*, 2nd ed.; Chapman, D., Ed.; UNESCO/WHO/UNEP: Nairobi, Kenya, 1992; pp. 239–316.

16. Chakrapani, G.J. Factors controlling variations in river sediment loads. *Curr. Sci. India* **2005**, *88*, 569–575.
17. Whipple, K.X.; Dibiase, R.A.; Crosby, B.T. Bedrock rivers. In *Fluvial Geomorphology*; Elsevier Inc.: Amsterdam, The Netherlands, 2013; pp. 550–573.
18. Miller, J.R.; Watkins, X.; O’Shea, T.; Atterholt, C. Controls on the Spatial Distribution of Trace Metal Concentrations along the Bedrock-Dominated South Fork New River, North Carolina. *Geosciences* **2021**, *11*, 519. [[CrossRef](#)]
19. Álvarez-Vázquez, M.A.; De Uña-Álvarez, E. Growth of sculpted forms in bedrock channels (Miño River, northwest Spain). *Curr. Sci. India* **2017**, *112*, 996–1002. [[CrossRef](#)]
20. Álvarez-Vázquez, M.A.; De Uña-Álvarez, E. Inventory and assessment of fluvial potholes to promote geoheritage sustainability (Miño River, NW Spain). *Geoheritage* **2017**, *9*, 549–560. [[CrossRef](#)]
21. Álvarez-Vázquez, M.Á.; De Uña-Álvarez, E. An exploratory study to test sediments trapped by potholes in Bedrock Rivers as environmental indicators (NW Iberian Massif). *Cuatern. Geomorfol.* **2021**, *35*, 59–77. [[CrossRef](#)]
22. Richardson, K.; Carling, P.A. *A Typology of Sculpted Forms in Open Bedrock Channels*; Geological Society of America: Boulder, CO, USA, 2005; Special Paper 392; 108p.
23. Barrera Morate, J.L.; González Lodeiro, F.; Marquínez García, J.; Martín Parra, L.M.; Martínez Catalán, J.R.; Pablo Maciá, J.G. *Memoria del Mapa Geológico de España, Escala 1:200.000, Ourense/Verín*; Instituto Tecnológico GeoMinero de España: Madrid, Spain, 1989; 284p.
24. Álvarez-Vázquez, M.A.; De Uña-Álvarez, E.; Prego, R. Background of U and Th in sediments of bedrock rivers. *Environ. Smoke* **2021**, 17–23. [[CrossRef](#)]
25. Grygar, T.M.; Popelka, J. Revisiting geochemical methods of distinguishing natural concentrations and pollution by risk elements in fluvial sediments. *J. Geochem. Explor.* **2016**, *170*, 39–57. [[CrossRef](#)]
26. Franklin, R.; Ferreira, F.; Bevilacqua, J.; Fávoro, D. Assessment of metals and trace elements in sediments from Rio Grande Reservoir, Brazil, by neutron activation analysis. *J. Radioanal. Nucl. Chem.* **2012**, *291*, 147–153. [[CrossRef](#)]
27. Boës, X.; Rydberg, J.; Martínez-Cortizas, A.; Bindler, R.; Renberg, I. Evaluation of conservative lithogenic elements (Ti, Zr, Al, and Rb) to study anthropogenic element enrichments in lake sediments. *J. Paleolimnol.* **2011**, *46*, 75–87. [[CrossRef](#)]
28. Bau, M.; Schmidt, K.; Pack, A.; Bendel, V.; Kraemer, D. The European Shale: An improved data set for normalisation of rare earth element and yttrium concentrations in environmental and biological samples from Europe. *Appl. Geochem.* **2018**, *90*, 142–149. [[CrossRef](#)]
29. McLennan, S.M. Lanthanide rare earths. In *Encyclopedia of Geochemistry*, 2nd ed.; White, W.M., Ed.; Springer: Berlin/Heidelberg, Germany, 2018. [[CrossRef](#)]
30. Taylor, S.; McLennan, S. *The Continental Crust: Its Composition and Evolution*; Blackwell Scientific Publications: Hoboken, NJ, USA, 1985; 312p.
31. Chen, H.; Chen, Z.; Chen, Z.; Ma, Q.; Zhang, Q. Rare earth elements in paddy fields from eroded granite hilly land in a southern China watershed. *PLoS ONE* **2019**, *14*, e0222330. [[CrossRef](#)]
32. Ramos, S.J.; Dinali, G.S.; Oliveira, C.; Martins, G.C.; Moreira, C.G.; Siqueira, J.O.; Guilherme, L.R. Rare earth elements in the soil environment. *Curr. Pollut. Rep.* **2016**, *2*, 28–50. [[CrossRef](#)]
33. Bayon, G.; Toucanne, S.; Skonieczny, C.; André, L.; Bermell, S.; Cheron, S.; Dennielou, B.; Etobleau, J.; Freslon, N.; Gauchery, T.; et al. Rare earth elements and neodymium isotopes in world river sediments revisited. *Geochim. Et Cosmochim. Acta* **2015**, *170*, 17–38. [[CrossRef](#)]
34. Prego, R.; Brito, P.; Álvarez-Vázquez, M.A.; Caetano, M. Lanthanides and yttrium in the sediments of the lower Minho River (NW Iberian Peninsula): Imprint of tributaries. *J. Soil Sediment* **2019**, *19*, 2558–2569. [[CrossRef](#)]
35. Ebrahimi, P.; Barbieri, M. Gadolinium as an emerging microcontaminant in water resources: Threats and opportunities. *Geosciences* **2019**, *9*, 93. [[CrossRef](#)]
36. Álvarez-Vázquez, M.A.; Hošek, M.; Elznicová, J.; Pacina, J.; Hron, K.; Fačevicová, K.; Talská, R.; Bábek, O.; Grygar, T.M. Separation of geochemical signals in fluvial sediments: New approaches to grain-size control and anthropogenic contamination. *Appl. Geochem.* **2020**, *123*, 104791. [[CrossRef](#)]